Active Damping Techniques for LCL-Filtered Inverters-Based Microgrids

Lorzadeh, Iman ; Firoozabadi, Mehdi Savaghebi; Askarian Abyaneh, Hossein; Guerrero, Josep M.

Published in:
Proceedings of the 2015 IEEE 10th International Symposium on Diagnostics for Electrical Machines, Power Electronics and Drives (SDEMPED)

DOI (link to publication from Publisher):
10.1109/DEMPED.2015.7303722

Publication date:
2015

Document Version
Early version, also known as pre-print

Active Damping Techniques for *LCL*-Filtered Inverters-Based Microgrids

Iman Lorzadeh, Mehdi Savaghebi, *Member, IEEE*, Hossein Askarian Abyaneh, *Senior Member, IEEE*, and Josep M. Guerrero, *Fellow, IEEE*

***Abstract* — *LCL*-type filters are widely used in grid-connected voltage source inverters, since it provides switching ripples reduction with lower cost and weight than the *L*-type counterpart. However, the inclusion of *LCL*-filters in voltage source inverters complicates the current control design regarding system stability issues; because an inherent resonance peak appears due to zero impedance at that resonance frequency. Moreover, in grid-interactive low-voltage microgrids, the interactions among the *LCL*-filtered-based parallel inverters may result in a more complex multi-resonance issue which may compromise the power quality and stability of the microgrid. Therefore, due to the effect of resonances on the system stability and power quality, this paper presents a state-of-the-art review of resonance characteristics and related issues in single- and multi-inverter-systems. Furthermore, this paper introduces the different active damping approaches for grid-connected inverters with *LCL* filters, which are based on high-order filters and additional feedbacks methods. These techniques are analyzed and discussed in detail.**

Index Terms — ***Active damping techniques; grid-interactive microgrid; LCL-filter***

I. INTRODUCTION

DUe to increasing adoption of electronically-interfaced distributed generation (DG) units in power distribution systems, control and design of voltage source inverters (VSIs) have become a very important issue for robust integration of DG units [1]. Control of interfacing converters is a flexible outstanding opportunity to achieve improved operation of DG units and to overcome various distribution system power quality problems [2]. Hence, the microgrid concept has been raised to attain better operation through coordinated control among parallel interface converters.

In low-power applications with high switching frequency, a single inductor *L* is usually installed in series with the output ports of the inverter to filter the switching harmonics. However, using such a simple topology in high-power applications with low switching frequency leads to the costly and bulky *L*-filters. In order to overcome these limitations, *LCL* low-pass filter is preferred to the *L*-type counterpart. Fig. 1 demonstrates a typical structure of three-phase VSI connected to grid/load through the popular types of the passive filters.

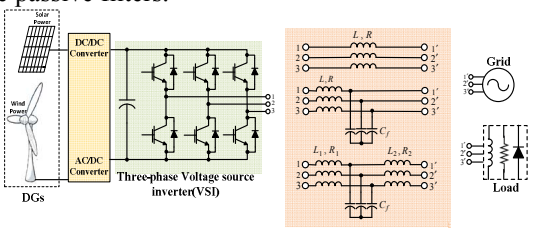

Fig.1. Three-Phase VSI connected to grid/load through *L*/*LC*/*LCL* filters.

Despite prominent merits of the *LCL*-filter over the *L*-filter, the incorporation of it with VSIs complicates the current control design to preserve the system stability. In fact, an inherent resonance peak appears at the frequency response owing to zero impedance at the resonance frequency [4], [5]. Therefore, these third-order passive filters introduce some resonance hazards at the frequency response, so that declines the efficiency and performance of the inverter system and even in the worst case, lead to system instability. Consequently, one of the most resonant issues in the VSIs-based microgrids is the inherent resonance caused by the inverter output *LCL*-filters which has mainly a fixed frequency due to the small variation range of the filter parameters.

On the other hand, in most cases, long feeders with nontrivial parasitic shunt capacitances (i.e., underground or submarine cable) [6], [7] and also presence of the shunt capacitor banks for local reactive power compensation, are ignored and for convenience of the VSI system analysis, the line has only been considered as a lumped inductance [8]. In fact, one can well understand that under these conditions, the distributed series inductances and shunt capacitances along a feeder may form an *LC* ladder network, which resulting in cause to amplify or increase the number of system resonance peaks, and can introduce current and voltage distortions and increase the risk of system instability. It means that greater challenges are brought to the system power quality by multiple resonances.

In addition, in a grid-interactive low voltage (LV) microgrid with multiple parallel *LCL*-filtered VSIs and relatively high upstream grid impedance, the interactions among parallel inverters can bring a more challenging resonance, which can also jeopardize the power quality and

This work was supported by the Technology Development and Demonstration Program (EUDP) through the Sino-Danish Project "Microgrid Technology Research and Demonstration" (meter.et.aau.dk).

I. Lorzadeh and H. Askarian Abyaneh are with Department of Electrical Engineering, Amirkabir University of Technology, Iran, (e-mail: lorzadeh@aut.ac.ir; askarian@aut.ac.ir).

M. Savaghebi and J. M. Guerrero are with the Department of Energy Technology, Aalborg University, 9220 Aalborg, Denmark,

stability of the microgrid. These interactions may cause severe harmonic currents in the inverters output even when the proper harmonic resonance damping schemes are adopted based on the single-inverter model [9].

Consequently, the adoption of proper resonance damping methods in order to achieve high power quality and ensure the system stability is indispensable. There are many well-established methods for shaving the resonance peaks, which can be classified as active damping (AD) and passive damping (PD) techniques. Hence, regarding the effect of resonances on the system stability and power quality, this paper conducts an in-depth investigation on the different resonance characteristics and issues in the microgrids dominated by *LCL*-filtered parallel inverters. In addition, different active resonance damping techniques will be discussed in detail.

TABLE I
TYPICAL FILTER PARAMETERS

Symbol	Quantity
f_0	50Hz
L_1	1.8mH
C_f	27μF
L_2	1.8mH
L_g	2.5mH
R_1,R_2	0.1Ω
Rg	0.4Ω

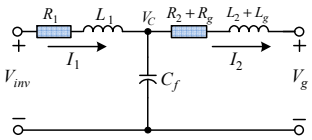

Fig.2. Grid-connected *LCL*-filter structure.

II. CLASSIFICATION OF ACTIVE RESONANCE DAMPING TECHNIQUES

Although effectiveness of the PD techniques have been proven, thanks to the significant advances in power electronic technologies, the switching frequency and control bandwidth of a DG interface inverter can be much higher than the resonant frequency of output filters, even for wind power converters at a few megawatts (MW) [10]. Consequently, AD schemes without any additional power losses is often considered as a more promising way to provide sufficient damping effects via improved control algorithms. However, it is provided at the expense of increased complexity of controller tuning. AD techniques can be classified into two categories. The first group includes schemes such as high-order controllers (filters) which do not require additional measurement [11]-[15]. Another group consists of extra feedback (multi-loop) based AD control approaches which use the feedback of filter capacitor current [4], [16], [17] or voltage [3], the virtual resistor scheme [9], [18], [19], and composite control method [20], [21]. It is clear that the implementation of the latter approaches needs additional sensors, which undoubtedly increase overall system cost and the complexity. In order to overcome this restriction, a number of estimation based sensor-less AD methods have been proposed [22], [23]. Nevertheless, the performance of these algorithms strongly depends on the several factors such as accuracy of sampling the inverter-side current [24], and the precision of system parameters and model [25].

III. SINGLE-INVERTER SYSTEM RESONSNCE CHARACTERISTICS AND CONTROL STARTEGY

A. Resonance in a single-inverter system

Fig. 2 shows a single-phase grid-connected *LCL*-filter structure which includes inverter-side inductance L_1, capacitor C_f, grid-side Inductance L_2, line (feeder) inductance L_g, equivalent series resistors (ESRs) R_1, R_2, and R_g, inverter output voltage V_{inv}, grid voltage V_g, inverter-side current I_1, grid-side current I_2, and capacitor voltage V_C. The typical filter parameters are present in Table I and, accordingly, it has the components as follows:

$$Z_1(s) = R_1 + L_1 s \tag{1}$$

$$Z_2(s) = 1/(C_f s) \tag{2}$$

$$Z_3(s) = (R_2 + R_g) + (L_2 + L_g)s \tag{3}$$

The relation between V_{inv}, V_g and system state variables for the aim of current control are easily obtained as follows:

$$G_{V_{inv}}^{I_2}(s) = \frac{I_2(s)}{V_{inv}(s)}\bigg|_{V_g=0} = \frac{Z_2(s)}{Z_1(s)Z_2(s) + Z_1(s)Z_3(s) + Z_2(s)Z_3(s)} \tag{4}$$

$$G_{V_g}^{I_2}(s) = \frac{I_2(s)}{V_g(s)}\bigg|_{V_g=0} = -\frac{Z_1(s)+Z_2(s)}{Z_1(s)Z_2(s)+Z_1(s)Z_3(s)+Z_2(s)Z_3(s)} \tag{5}$$

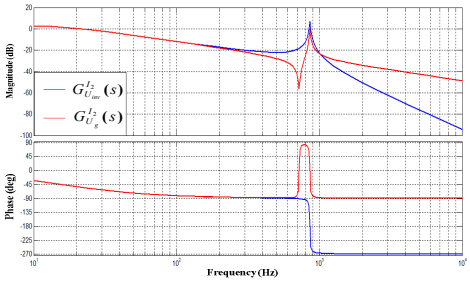

Fig.3. Bode plots of transfer functions of the *LCL*-filter for current-controlled VSI system.

Fig. 3 illustrates the Bode plots of above transfer functions for current-controlled VSI system. As is evident in the Fig. 3, when a VSI is terminated with an *LCL*-filter, there will be a resonance peak in the gain response of system at the natural resonance frequency of the filter, even if the ESRs of passive components are included. Thus, the design of suitable current control strategies as well as efficient damping controller in order to avoid the resonance peaks and maintain closed-loop system stability are essential. The output current of the *LCL*-filter is resonated at the internal resonance frequency as follows:

$$f_{res} = \frac{\omega_{res}}{2\pi} = \sqrt{\frac{1}{C_f} \cdot \left(\frac{1}{L_1} + \frac{1}{(L_2 + L_g)} \right)} \tag{6}$$

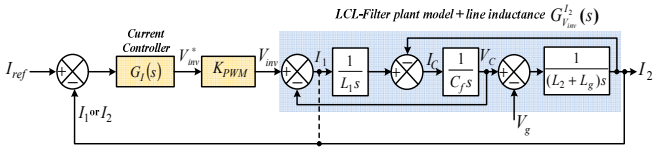

Fig.4. Block diagram of single-loop current control scheme by using grid-side or inverter-side current feedback.

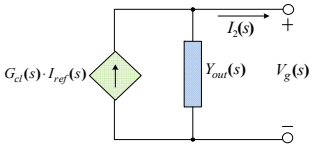

Fig.5. The Norton's equivalent circuit of current-controlled VSI.

B. Conventional single-loop control strategy

In the grid-connected VSIs with *LCL*-filters, in order to regulate the current injected to the grid directly or indirectly, there is flexibility in the choice of the current feedback for the current controller compared with those that linked solely with *L*-filter. It means that either inverter-side current or grid-side current or even their weighted average current (WAC) value [26]-[28] may be sensed. Fig. 4 shows the single-loop current control block diagram for *LCL*-filter-based VSIs. The control open-loop gain for the system of Fig. 4 can be easily derived as

$$G_{open\_loop}(s) = G_I(s) \cdot G_{V_{inv}}^{I_2}(s) \tag{7}$$

where, G_I (s) is current controller. Moreover, the steady-state error can be defined as

$$E(s) = \frac{I_{ref}(s)}{1 + G_{open\_loop}(s)} \tag{8}$$

For the single-loop current control shown in Fig 4, the filter plant can be expressed as follows:

$$I_2(s) = G_{V_{inv}}^{I_2}(s) \cdot V_{inv}(s) + G_{V_g}^{I_2}(s) \cdot V_g(s) \tag{9}$$

On the other hand, the resulting inverter voltage in (9) is obtained easily as follows:

$$V_{inv}(s) = G_I(s) \cdot \left(I_{ref}(s) - I_2(s) \right) \tag{10}$$

As a result, the closed-loop Norton's equivalent circuit can be achieved by replacing (10) in (9) as

$$I_2(s) = G_{cl}(s) \cdot I_{ref}(s) - Y_{out}(s) \cdot V_g(s) =$$

$$\frac{G_{open\_loop}(s)}{1 + G_{open\_loop}(s)} \cdot I_{ref}(s) + \frac{G_{V_g}^{I_2}(s)}{1 + G_{open\_loop}(s)} \cdot V_g(s) \tag{11}$$

Thus, the Norton's equivalent circuit of single-loop current-controlled VSI with the *LCL*-filter is as shown in Fig. 5. This circuit is useful for evaluating multiple resonances of parallel inverters, which will be discussed in Section VI.

Tang *et al*. [25] have shown that in current-controlled grid-connected VSIs, the single-loop current control method based on the inverter-side current feedback is more stable than the grid-side current feedback due to the addition of an intrinsic damping term to the control loop, which is not provided by the grid-side current feedback.

Generally, in conventional single-loop control strategy to mitigate the resonance peak amplitude under 0 dB to closed-loop system stability, the open-loop control gain is necessary to be quite small and this will lead to an increase in steady-state tracking error of the sinusoidal reference (see (8)). In addition, the single-loop control schemes suffer from low-bandwidth and grid background harmonics as well as control dynamics and steady-state performance restrict each other [24].

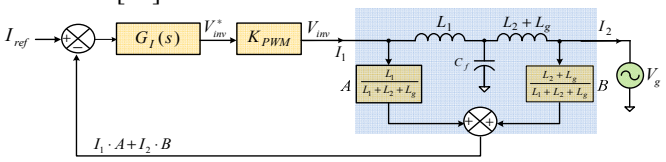

Fig.6. Block diagram of *LCCL* control strategy.

C. LCCL control strategy

In [28] a new single-loop current feedback strategy has been proposed for *LCL*-filter-based grid-connected inverter. This scheme is shown in Fig. 6. As illustrated, by splitting the capacitor of the *LCL*-filter C_f into two parts, proportional to the inductances values of the capacitor's two sides, to form a *LCCL* filter, the current flowing between these two capacitors is sensed and considered as the feedback for the current controller. Therefore, the proposed strategy can provide damping to the VSI system by degrading the filter transfer function (that is from V_{inv} to current $I_{1,2}$) from a third-order to a first-order similar to an *L*-type filter. As a result, it can offer a higher control gain and thus remove the low bandwidth limitation and steady-state error of sinusoidal reference tracking in conventional single-loop control. However, the control system design depends on *LCL*-filter physical parameters, so the damping performance is more sensitive to system parameters change.

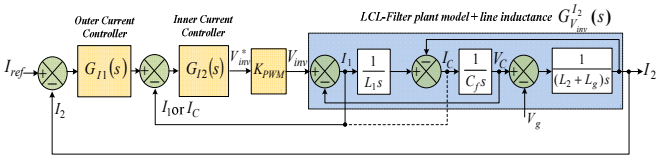

Fig.7. Block diagram of cascaded double-loop current control scheme.

IV. Active Damping Based on Additional Feddbacks

A. Cascaded double-loop control

To deal with the limitations of traditional single-loop control, the cascaded double-loop control scheme with more measurements is introduced as illustrated in Fig. 7. This scheme can also inherently provide damping effects to filter plant of VSI inverter. As it can be seen in Fig. 7, the control scheme consists of an outer controller and an inner controller. According to the Fig. 7, the pulse width modulation (PWM) reference signal can be easily obtained

as follows:

$$V_{inv}(s) = G_{I1}(s) \cdot G_{I2}(s)(I_{ref}(s) - I_2(s)) - G_{I2}(s) \cdot I_{Internal}(s) \quad (12)$$

where $I_{Internal}$(s) is the inner loop feedback variable which can be either the capacitor current or inverter-side inductor current. The inner controller G_{I2}(s) provides damping effects to the filter circuit by modifying the inverter reference signal directly. In [17] the performance of two active damping approaches for PI-based current control VSI with *LCL*-filter has been analyzed and compared under various resonance frequencies. It has been shown that in high resonance frequencies, the system is stable only with proportional feedback of the capacitor current, at medium resonance frequencies, both methods present good performance, and at low resonance frequencies, both approaches lead to system instability.

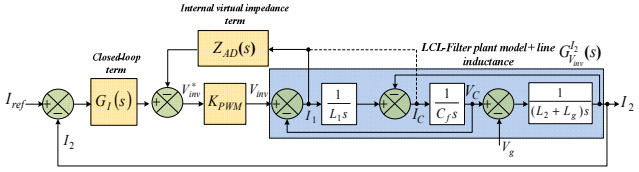

Fig.8. Block diagram of GCC control scheme.

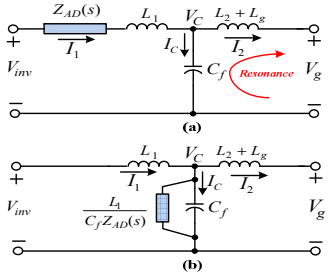

Fig.9. Internal virtual damping impedance (a) with inverter-side inductor current feedback, (b) with capacitor current feedback.

B. Virtual resistance-based active damping scheme

This scheme is realized by applying additional control loops in order to emulate a physical resistor but without the associated losses. A generalized closed-loop control (GCC) scheme has been proposed for VSIs with *LC-LCL* output filters [18] as demonstrated in Fig. 8. As illustrated, it has a single-loop control term related to inverter output current and an internal virtual impedance term, which unlike the conventional cascaded double-loop control, each term can be controlled independently. Using the GCC scheme provides a well dampened filter circuit at first and then based on the modified filter plant, the closed-loop term G_I(s) can be designed in order to provide a better reference tracking control. Thus, in this case, the PWM reference signal of VSI expressed as follows:

$$V_{inv}(s) = G_I(s) \cdot \left(I_{ref}(s) - I_2(s)\right) - Z_{AD}(s) \cdot I_{Internal}(s) \quad (13)$$

The internal virtual impedance term is similar to the inner control loop of a double-loop control (see (12)), which is able to provide sufficient damping effect to the VSI system through adding a virtual damping impedance to the main filter plant.

When the inductor current I_1 is considered as the feedback variable, the internal virtual impedance term Z_{AD}(s) is placed in series with the inverter-side inductance, because it makes an additional voltage drop at the PWM voltage, as demonstrated in Fig. 9(a). It is evident that if just a proportional controller is employed for Z_{AD} (s), the internal virtual damping term will be a damping resistor. It should be noted that if a large damping impedance term is added to filter circuit, it will introduce an additional *LC* resonance between C_f and grid-side inductor due to blocking of the left side of the *LCL* filter. It can easily be seen in Fig. 9(a). In addition, a large damping impedance term will significantly reduce the magnitude of $G_{V_{inv}}^{I_2}(s)$ and result in poor dynamic tracking performance.

In the contrary, if the capacitor current is considered as the internal term feedback, it will have a different physical meaning due to presence of inverter-side inductor between the inverter output voltage and the filter capacitor branch. This can easily be determined by obtaining the output current of filter I_2 around the resonance frequency at the circuit of Fig. 2 regardless ESRs and when the internal virtual impedance term is applied, as follows

$$I_2(s) = I_1(s) - I_C(s) = -\left(\frac{G_I(s) \cdot V_C(s) + V_C(s) + Z_{AD}(s) \cdot I_C(s)}{sL_1} + sC_f V_C(s)\right)$$

$$= -\left(\frac{G_I(s)}{sL_1} + \frac{V_C(s)}{sL_1} + sC_f V_C(s) + \frac{Z_{AD}(s) C_f(s) V_C(s)}{L_1}\right) \quad (14)$$

Further looking into (14) reveals that the active damping based on capacitor current introduces an extra term to output current, which can be modeled as a parallel impedance with the filter capacitor as shown in Fig. 9(b). As illustrated from Fig. 9(b) the limitations about setting the virtual damping term Z_{AD} (s) in the inductor current feedback case, will not be present in this situation. Therefore, the capacitor current feedback can present better dynamic performance in introduction of the virtual damping term compared to inverter-side inductance current feedback.

C. Active damping based on grid-side current feedback only

In [24], an AD method using only the feedback of the grid side current has been proposed for current-controlled *LCL*-terminated inverters considering the relationship between the capacitor and grid-side currents. For achieving this, the signal flow graph and response-fitting methods are applied. The aim of this scheme is to reduce the cost associated with the use of precise sensors of the extra feedback methods. At first, by using the signal flow graph method, the capacitor current feedback is transformed to only the grid-side current feedback. Meanwhile, the grid voltage feedback also appears in this transformation, but its effect has been removed due to the amplification of grid background voltage harmonics on the inverter voltage (see Fig. 10(a)). As seen in Fig. 10(a), a second-order derivative

filter is required to remove the resonance. Since the implantation of this filter is difficult and leads to the amplification of harmonics at frequencies around the switching frequency, a first-order high-pass filter has been proposed instead of the second-order derivative filter by using the response-fitting method. This approach is shown in Fig. 10(b). Although this method only uses one current sensor, setting of the filter parameters to achieve better damping performance and the system stability is difficult, since the filter parameters restrict each other.

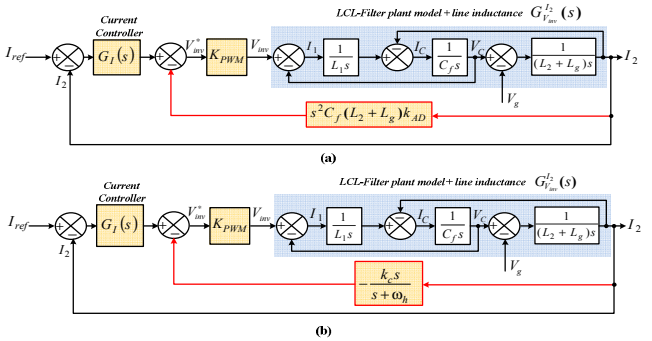

Fig.10. AD based on with only grid-current feedback (a)control structure, (b)by using a first-order high-pass filter.

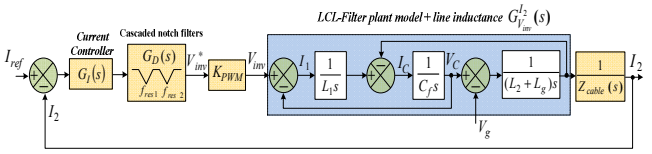

Fig.11. Block diagram of a filter-based AD method for a long cable-based grid-connected VSI system.

V. FILTER-BASED ACTIVE DAMPING METHODS

A. Overview

In the filter-based AD methods, a high-order filter is added in cascade with the system controller. Second-order low-pass, notch, and lead-leg filters can be applied. Thus the response around the resonance frequency can be changed for damping of unstable dynamics, so that the controller can preserve suitable stability margins. Although in filter-based AD methods the additional sensors are not required and the stability is improved, but the bandwidth which is also very important, greatly reduced and the robustness and dynamic still need further investigation. To understand more about this method, in the next sub-section typically a notch-filter-based AD approach will be presented for a grid-connected VSI with long cable [12].

B. Notch-filter-based active damping approach

As mentioned before, according to the distributed model for long cable or feeder [30], [31], several significant resonance peaks (in other words, numerous poles and zeros on the imaginary axis) can be made in the open loop transfer function of the parallel-grid interactive inverter system due to the high-order *LC* configuration. It should be pointed out that in this case, the use of extra feedback based AD techniques is a little more difficult than filter based methods because of the unknown voltage or current inside cable. A filter-based AD method according to a cascaded notch-filter (multiple notch filters in series) has been proposed in [12] to eliminate the low frequency resonances introduced by the long cable of a grid-connected DG system. Block diagram of the proposed control method for a current-controlled DG inverter is shown in Fig. 11. $G_D(s)$ is a cascaded notch filter which its center frequencies has been tried to be consistent with the cable resonance peaks to damp resonant gains due to its reject-band filter characteristic and $Z_{cable}(s)$ is input impedance of the cable assuming that the cable is terminated with an voltage source, which can be defined as follows [8]

$$Z_{cable}(s) = Z_C \cdot \frac{Z + \tanh(\gamma l)}{Z \tanh(\gamma l) + 1} \tag{15}$$

where $Z = Z_g / Z_C$. Z_g is the impedance seen from the grid-side, $Z_C = \sqrt{z/y}$ is the characteristic impedance of the feeder, and $\gamma = \sqrt{z \cdot y}$ is the propagation constant. $z = R + j\omega L$ and $y = j\omega C$, respectively, are the series impedance and shunt capacitance of the cable in per-unit length or per kilometer. However, the robustness and performance of the cascaded notch filter-based AD method [12] is poor, because the specified resonance frequencies for the filter are closely related to cable parameters.

VI. INVESTIGATION OF MULTIPLE RESONANCE PARALLEL INVERTER-BASED MICROGRIDS

A. Discription problem

Most of the existing resonance analyses in the literature are mainly focused on single grid-connected inverter system. However, unlike the single-inverter system in which the resonance frequency is commonly fixed, in parallel-inverters-based microgrids, greater resonance challenges at various frequencies resulting from mutual interactions between parallel inverters may appear [9], [14], [32], and [33]. These interactions may cause severe harmonic currents in the inverters output even when the suitable harmonic resonance damping schemes are designed based on the single-inverter model [9]. In the grid-connected microgrid operation with a stiff PCC voltage, each inverter is considered to be separated from other inverters. It means that a single-inverter model may be acceptable for system study. Nevertheless, the single-inverter model cannot describe the behavior of a microgrid, especially, in order to analyze the multiple resonances among parallel inverters, mainly in LV microgrid with higher upstream grid impedance [9]. Therefore, for exact study of multiple resonances among parallel-inverter units, a microgrid model involving all the factors that determine the resonance issues in the system should be developed. A simplified circuit model has been presented in [32], to study the resonance interactions without considering the effects of DG

controllers. In [33] an equivalent circuit based on the open-loop transfer functions has been also developed to investigate multiple resonances. However, considering that the current references of current-controlled inverters are normally controlled independently, the proposed method in [33] cannot explain the transient behavior of the microgrid [9].

B. Investigation of multiple resonances

This sub-section presents a microgrid model based on the closed-loop Norton's equivalent circuit for evaluation of the multiple resonance problems in the multiple-parallel *LCL*-filtered inverters [33]. The configuration of a microgrid with N parallel *LCL*-filtered inverters and a capacitor which is typically connected to the common bus for local reactive power compensation is illustrated in Fig. 12. The grid voltage V_g(s) is connected to PCC through its related series impedance Z_g(s). The equivalent circuit of such a microgrid can be achieved by replacing each inverter with its corresponding current source circuit model in Fig. 5, as shown in Fig.13. Y_g(s) is the grid series admittance which can be obtained as 1 / Z_g(s) and Y_Q is $j\omega C_Q$.

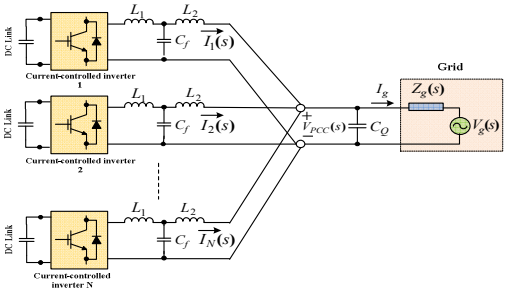

Fig.12. Configuration of a microgrid with multiple-parallel *LCL*-filtered inverters.

According to the model of Fig. 13, the grid-side current of the inverters can be determined by utilizing Kirchhoff's law. For instance, the grid-side current of inverter 1, I_1(s), is obtained as follows:

$$I_1(s) = G_{cl,1}(s) \cdot I_{ref,1}(s) - V_{PCC}(s) \cdot Y_{out,1}(s) \tag{16}$$

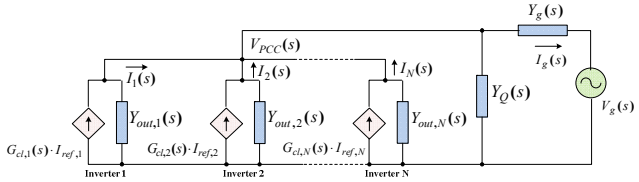

Fig.13. Closed-loop Norton's equivalent circuit of multiple-parallel *LCL*-filtered current-controlled inverters.

where

$$V_{PCC}(s) = \frac{\sum_{i=1}^{N} G_{cl,i}(s) \cdot I_{ref,i}(s) + Y_g(s) \cdot V_g(s)}{\sum_{i=1}^{N} Y_{out,i}(s) + Y_Q(s) + Y_g(s)} \tag{17}$$

Thus, the grid-side current of inverter 1 can be easily derived from (16) and (17). The grid-side currents of other inverters can be calculated with a similar analysis. As a result, the interaction effects of multiple-parallel inverters in the microgrid can be described as follows using a closed-loop transfer function matrix [9] by taking the grid voltage and reference current as inputs and grid-side currents of inverters as outputs:

$$\begin{bmatrix} I_1(s) \\ I_2(s) \\ .. \\ I_N(s) \end{bmatrix} = \begin{bmatrix} F_1(s) & M_{12}(s) & .. & M_{1N}(s) \\ F_{21}(s) & F_2(s) & .. & M_{2N}(s) \\ .. & .. & .. & .. \\ F_{N1}(s) & F_{N2}(s) & .. & F_N(s) \end{bmatrix} \cdot \begin{bmatrix} I_{ref,1}(s) \\ I_{ref,2}(s) \\ .. \\ I_{ref,N}(s) \end{bmatrix} - \begin{bmatrix} W_1 \\ W_2 \\ .. \\ W_N \end{bmatrix} \cdot V_g(s) \tag{18}$$

where the elements of (18) can be derived as

$$F_j(s) = G_{cl,j}(s) - \frac{Y_{out,j}(s) \cdot G_{cl,j}(s)}{\sum_{i=1}^{N} Y_{out,i}(s) + Y_Q(s) + Y_g(s)} \tag{19}$$

$$M_{jt}(s) = -\frac{Y_{out,j}(s) \cdot G_{cl,t}(s)}{\sum_{i=1}^{N} Y_{out,i}(s) + Y_Q(s) + Y_g(s)} \tag{20}$$

$$W_j(s) = \frac{Y_{out,j}(s) \cdot Y_g(s)}{\sum_{i=1}^{N} Y_{out,i}(s) + Y_Q(s) + Y_g(s)}, \; j \neq t, j, t \in [1, N] \tag{21}$$

It is clear from the above equations that unlike the single current-controlled inverter system, a grid-interactive microgrid with multiple-parallel inverters has three independent resonance terms for each inverter. Term F_j (s) presents the resonance introduced by each inverter, which may be excited by the reference current change of the inverter itself, and consequently, the grid-side current of the inverter can have serious resonant harmonic currents. The second resonance term M_{jt} (s) for each inverter is related to the interaction among inverters, which may be excited by a reference current change of other inverters. This term can introduce considerable transient harmonic currents during the step change of the reference currents of other inverters similar to the first one. Finally, the resonance term W_j (s) represents the interaction between the main grid and the inverters of microgrid, which can be excited by the grid transient and steady-state background harmonics disturbances. Consequently, according to the analytical descriptions abovementioned, in a LV microgrid with intense inverter coupling due to high grid impedance, and without suitable resonance damping, the grid-side currents of the parallel inverters can be strongly distorted. Thus, the power quality of the microgrid is compromised. Moreover, in [10] an AD method using virtual-harmonic resistance has been proposed based on a deadbeat current controller to suppress the multiple resonances. However, control of virtual impedance is more sensitive to the mismatched line and grid impedances and system parameter variations. In addition, the sampling and control delays may have impacts on efficacy of deadbeat control scheme. Therefore, applying of various active damping methods to deal with the multiple resonances in a parallel inverter-based grid-interactive microgrid such as transient and steady-state resonances still require further investigations.

VII. CONCLUSION

This paper presents a general review of the resonances introduced by *LCL*-filter in a single-inverter system, and

interactive effects among multiple-parallel inverters in a grid-interactive microgrid. Using a closed-loop Norton's equivalent circuit of multiple-parallel inverters in a microgrid, it has been shown that there will be multiple resonances which can be excited by the reference current change of the inverters, the grid transient and steady-state background harmonics disturbances. In addition, the active damping methods have been studied in detail.

REFERENCES

[1] J. M. Carrasco, L. G. Franquelo, J. T. Bialasiewwicz, E. Galvan, R. C. P. Guisado, M. A. M. Prats, J. I. Leon, and N. Moreno-Alfonso, "Power-Electronic systems for the grid integration of renewable energy sources: A survey," *IEEE Trans. Ind. Electron.*, vol. 53, no. 4, pp. 1002-1016, Aug. 2006.

[2] M. Savaghebi, A. Jalilian, J. C. Vasquez, J.M. Guerrero, "Secondary Control Scheme for Voltage Unbalance Compensation in an Islanded Droop-Controlled Microgrid," IEEE Trans. Smart Grid., vol. 3, pp. 797-807, Feb. 2012.

[3] I. J. Gabe, V. F. Montagner, and H. Pinheiro, "Design and implementation of a robust current controller for VSI connected to the grid through an LCL-filter," IEEE Trans. Power Electron., vol. 24, no. 6, pp. 1444–1452, Jun. 2009.

[4] Twining Erika and D. G. Holmes, "Grid current regulation of a three-phase voltage source inverter with an LCL input filter," IEEE Trans. Power Electron., vol. 18, no. 3, pp. 888–895, May 2003.

[5] J. Dannehl, C.Wessels, and F. W. Fuchs, "Limitations of voltage-oriented PI current control of grid-connected PWM rectifiers with LCL filters," IEEE Trans. Ind. Electron., vol. 56, no. 2, pp. 380–388, Feb. 2009.

[6] C. J. Chou, Y. K. Wu, G. Y. Han, and C. Y. Lee, "Comparative evaluation of the HVDC and HVAC links integrated in a large offshore wind farm: An actual case study in Taiwan," IEEE Trans. Ind. Appl., vol. 48, no. 5, pp. 1639–1648, Sep./Oct. 2008.

[7] C. C. Hsin and R. Bucknall, "Harmonic calculations of proximity effect on impedance characteristics in subsea power transmission cables," IEEE Trans. Power Delivery., vol. 24, no. 4, pp. 2150–2158, Jul./Aug. 2009.

[8] J. W. Phinney, D. J. Perreault, and J. H. Lang, "Synthesis of lumped transmission-line analogs," IEEE Trans. Power Electron., vol. 22, no. 4, pp. 1531–1542, Jul. 2007.

[9] J. He, Y. W. Li, D. Bosnjak, and B. Harris, "Investigation and active damping of multiple resonances in a parallel-inverter-based microgrid," IEEE Trans. Power Electron., vol. 28, no. 1, pp. 234–246, Jan. 2013.

[10] A. A. Rockhill, M. Liserre, R. Teodorescu, and P. Rodriguez, "Grid-filter design for a multi-megawatt medium-voltage voltage-source inverter," IEEE Trans. Ind. Electron., vol. 58, no. 4, pp. 1205–1217, Apr. 2011.

[11] J. Dannehl, M. Liserre, and F. W. Fuchs, "Filter-based active damping of voltage source converters with LCL filter," IEEE Trans. Ind. Electron., vol. 58, no. 8, pp. 3623–3633, Aug. 2011.

[12] S. Zhang, S. Jiang, X. Lu, B. Ge, and F. Z. Peng, "Resonance issues and damping techniques for grid-connected inverters with long transmission cable," IEEE Trans. Power Electron., vol. 29, no. 1, pp. 110–120, Jan. 2014.

[13] M. Liserre, R. Teodorescu, and F. Blaabjerg, "Stability of photovoltaic and wind turbine grid-connected inverters for a large set of grid impedance values," IEEE Trans. Ind. Appl., vol. 42, no. 5, pp. 1146–1154, Sep./Oct. 2006.

[14] X. Lu, K. Sun, L. Huang, M. Liserre, and F. Blaabjerg "An active damping method based on biquad digital filter for parallel grid-interfacing inverters with LCL filters," Applied Power Electron. Conf. and Expos. (APEC), pp. 392–397, 2014.

[15] R. P. Alzola, M. Liserre, F. Belaabjerg, R. Sebastian, J. Dannehl, and W. F. Fuches, "Systematic design of the lead-leg network method for active damping in LCL-filter based three-phase converters," IEEE Trans. Ind. Inform., vol. 10, no. 1, pp. 43–52, Feb. 2014.

[16] F. Liu, S. Duan, J. Yin, B. Liu, and F. Liu, "Parameter design of a two current-loop controller used in a grid-connected inverter system with LCL filter," IEEE Trans. Ind. Electron., vol. 56, no. 11, pp. 4483–4491, Nov. 2009.

[17] J. Dannehl, F. W. Fuchs, S. Hansen, and P. B. Thøgersen "Investigation of active damping approaches for PI-based current control of grid-connected pulse width modulation converters with LCL filters," IEEE Trans. Ind. Apl., vol. 46, no. 4, pp. 1509–1517, Jul/Aug. 2010.

[18] J. He, Y. and W. Li, "Generalized closed-loop control schemes with embedded virtual impedances for voltage source converters with LC or LCL filters," IEEE Trans. Power Electron., vol. 27, no. 4, pp. 1850–1861, Apr. 2012.

[19] Y. W. Li, "Control and resonance damping of voltage source and current source converters with LC filters," IEEE Trans. Ind. Electron., vol. 56, pp. 1511–1521, May 2009.

[20] E. Wu and P. W. Lehn, "Digital current control of a voltage source converter with active damping of LCL resonance," IEEE Trans. Power Electron., vol. 21, no. 5, pp. 1364–1373, Sep. 2006.

[21] J. R. Massing, M. Stefanello, H. A. Grundling, and H. Pinheiro, "Adaptive current control for grid-connected converters with LCL filter," IEEE Trans. Ind. Electron., vol. 59, no. 12, pp. 4681–4693, Dec. 2012.

[22] M. Malinowski and S. Bernet, "A simple voltage sensor-less active damping scheme for three-phase PWM converters with an LCL-filter," IEEE Trans. Ind. Electron., vol. 55, no. 4, pp. 1876–1880, Apr. 2008.

[23] S. Mariethoz and M. Morari, "Explicit model-predictive control of a PWM inverter with an LCL-filter," IEEE Trans. Ind. Electron., vol. 56, no. 2, pp. 389–399, Feb. 2009.

[24] J. Xu, S. Xie, and T. Tang, "Active damping-based control for grid-connected LCL-filtered inverter with injected grid current feedback only," IEEE Trans. Ind. Electron., vol. 61, no. 9, pp. 4746–4758, Sep. 2014.

[25] Y. Tang, P. C. Loh, P. Wang, F. H. Choo, and F. Gao, "Exploring inherent damping characteristic of LCL-Filters for three-Phase grid-connected," IEEE Trans. Power Electron., vol. 27, no. 3, pp. 1433–1442, Mar. 2012.

[26] Shen Guoqiao, Xu Dehong, Cao Luping, and Zhu Xuancai, "An improved control strategy for grid-connected voltage source inverters with an LCL filter," IEEE Trans. Power Electron., vol. 23, no. 4, pp. 1899–1906, Jul. 2008.

[27] G. Shen, X. Zhu, J. Zhang, and D. Xu, "A new feedback method for PR current control of LCL-filter-based grid-connected inverter," IEEE Trans. Ind. Electron., vol. 57, no. 6, pp. 2033–2041, Jun. 2010.

[28] N. He, D. Xu, Y. Zhu, J. Zhung, G. Shen, Y. Zhang, J. Ma, and C. Liu, "Weighted average current control in a three-phase grid inverter with an LCL filter," IEEE Trans. Power Electron., vol. 28, no. 6, pp. 2785–2797, June. 2013.

[29] P. A. Dahono, Y. R. Bahar, T. Sato, T. Kataoka, "Damping of transient oscillation on the output LC filter of PWM inverters by using a virtual resistor," in Proc. IEEE Power Electron. Drive Syst., pp. 403-407, 2001.

[30] K. Wada, H. Fujita, and H. Akagi, "Consideration of a shunt active filter based on voltage detection for installation on a long distribution feeder," IEEE Trans. Ind. Appl., vol. 38, no. 4, pp. 1123–1130, Jul./Aug. 2002.

[31] T.-L. Lee, J.-C. Li, and P.-T. Cheng, "Discrete frequency-tuning active filter for power system harmonics," IEEE Trans. Power Electron., vol. 24, no. 5, pp. 1209–1217, Apr. 2009.

[32] J. Enslin and P. Heskes, "Harmonic interaction between a large number of distributed power inverters and the distribution network," IEEE Trans. on Power Electronics, vol. 19, No. 6, pp. 1586-1593, 2004.

[33] J.L. Agorreta, M. Borrega, J. Lopez and L. Marroyo, "Modeling and control of N-paralleled grid-connected inverters with LCL filter coupled due to grid impedance in PV plants," IEEE Trans. On Power Electronics, Vol.26, No.3, pp. 770-785, 2011.